

The Effect of Cristobalite Seed on the Crystallization of Fused Silica Based Ceramic Core — A Kinetic Study

Ling-Yi Wang & Min-Hsiung Hon

Department of Materials Science and Engineering (MAT32), National Cheng Kung University, Tainan, Taiwan

(Received 10 December 1993; accepted 3 March 1994)

Abstract: Cristobalite-fused silica powder was prepared from a mixture of fused silica and cristobalite seed with a high-speed stirrer at 2400 r.p.m. for five minutes. Mixtures were then heated to the soaking temperature, between 1275°C and 1350°C, for different time periods. The formation of cristobalite was determined by a quantitative X-ray diffraction (QXRD). Cristobalite, as a phase transformation inhibitor, could affect the rate of transformation of fused silica to cristobalite. In the initial stage of the heating, the presence of cristobalite seed assists the crystallization of fused silica. However, it retards the crystallization as the soaking time is increased. The evidence shows that the cristobalite seed could induce a compressive stress due to the abrupt volume increase as cristobalite transformed from α phase to β phase at elevated temperature. From the kinetic analysis, the time exponent, n , decreases with increasing cristobalite seed additions, suggesting that the transformation kinetics is controlled by a long-range diffusion mechanism from a two-dimensional plate-like growth to a one dimensional needle-like growth. The activation energy calculation shows that the nucleation and growth process of cristobalite crystals is not similar to the incubation process of cristobalite nucleation in the solid-state reaction of fused silica-cristobalite.

1 INTRODUCTION

The single-crystal casting process has been capable of incorporating significant improvements in internal turbine airfoil cooling designs, and promoting the efficiency of turbine engine. This involves the manufacture of thinner, more delicate ceramic cores (Fig. 1). Ceramic cores are high technology parts produced by an injection molding process¹ which involves very precise and often complex forming tools to achieve 'near net shape'.

The properties of ceramic cores have to be finely balanced in order to produce acceptable dimensions in the cast blade or vane. A list of possible ceramic materials is reduced to only a few candidates due to the required chemical solubility. For the practice of single-crystal casting, the ceramics available are basic silica or silica/zircon based materials for the majority of nickel and

cobalt based superalloys. However, vendors frequently add appreciable amounts of cristobalite and occasionally some alumina. Huseby *et al.*² investigated six different commercial cores from four different vendors, in which about 0–37 vol% cristobalite phases were determined. Kato and Nozaki^{3,4} reported that the silica based ceramic cover material consisting of 10–20 wt% cristobalite could be applied for the directional solidification casting. It restrains softening of the core at high temperature and shrinkage of the core after reburning. Takayanagi and Katashima⁵ studied the crystallization of the fused silica flour, indicating that the crystallization control of fused silica is the most important for preventing the hot deformation of the ceramic core used to make the hollow-shaped investment casting. Mills and Chem⁶ showed the relationship between cristobalite level and the bend rate of the core test piece at 1150°C,

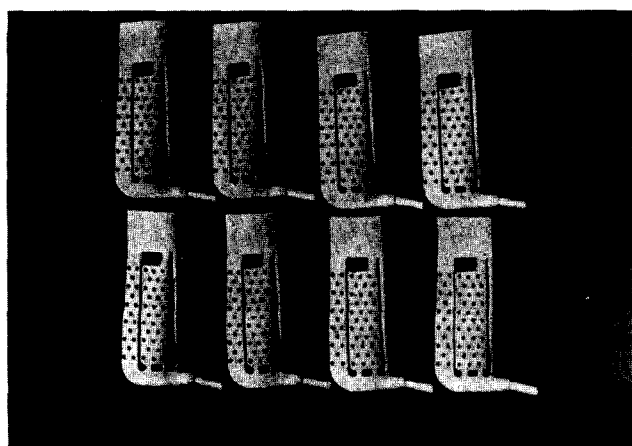


Fig. 1. Preformed ceramic core for single-crystal turbine blades application.

indicating that with a little devitrification the core had a very low level of cristobalite. These cores show poor refractoriness and cause excessive bowing in thin, delicate shapes for single-crystal cast hollow blades and vanes. Other work indicated core strength reduction with high levels of devitrification and about 60 wt% cristobalite.

A previous study,⁷ showed that zircon, as a phase transformation inhibitor, could effect the rate of transformation of fused silica to cristobalite. The purpose of this study is to investigate the phase transformation kinetics of fused silica to cristobalite in the system of cristobalite-fused silica as single crystal casting core materials.

2 EXPERIMENTAL PROCEDURE

2.1 Sample preparation

The raw materials used in this experiment are fused silica from the Combustion Engineering Co. (USA) for the grade with the commercial designation TECO-SILTM, and cristobalite powders from the Harbison-Walker Refractories Industries, Inc. (USA).

Two composition series of (1) Al: 100 wt% fused silica; and (2) Cl: 80 wt% fused silica + 20wt% cristobalite were investigated. The average particle size and surface area of samples are listed in Table 1.

Table 1. Composition and character of raw materials of ceramic cores for the single-crystal casting

Composition	Fused silica (wt%)	Cristobalite (wt%)	Average particle size (μm)	Surface area (m^2/g)
Al	100	0	13.80	4.55
Cl	80	20	14.65	4.24

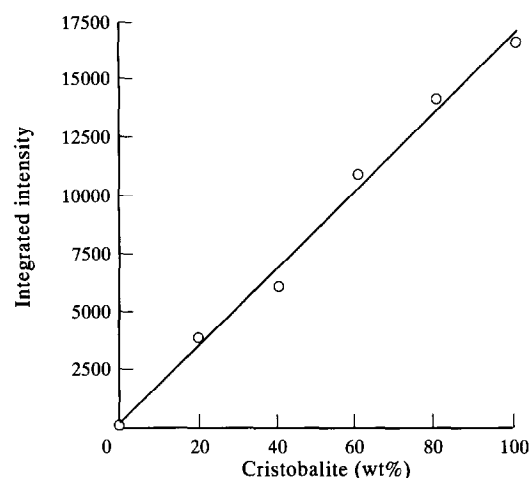


Fig. 2. The crystallinity calibration curve for cristobalite.

Raw materials were mixed with a high-speed stirrer at 2400 r.p.m. for about five minutes. Mixtures were then heated to temperatures between 1275°C and 1350°C, and held for different time periods. Afterwards, samples were air quenched and subsequently ground in an agate mortar. The sieved fraction (-200 mesh) of the ground powder was used for the quantitative determination of the transformation by X-ray diffraction analysis.

2.2 Quantitative X-ray diffraction analysis

X-Ray diffraction analysis, by the powder method, was conducted using a Rigaku D-Max/III V diffractometer, furnished with a 0.40 degree slit, a 0.05 degree detector, and nickel filter. Copper radiation K_{α} was used in all cases.

Standard cristobalite was prepared by firing commercial fused silica at 1550°C for 24 h. Then it was cooled, lightly ground and heated for another 24 h, with intermediate grinding, to produce cristobalite with relatively high purity. Devitrification generally occurred on the surface of the silica grains and grinding was necessary to expose the unconverted fused silica, prior to refiring. The calibration curve of compositions vs X-ray peak integrated intensity was obtained by using mixtures of cristobalite and fused silica in different proportions, as shown in Fig. 2. The peak selected for calibration was the strongest one ($d_{101} = 4.05\text{\AA}$), and external standards of the encountered crystalline phase.

3 RESULTS AND DISCUSSION

The results of quantitative X-ray diffraction of the samples which were isothermally annealed for various times were shown in Tables 2 and 3. It is interesting to note that all of the samples give a typical S-shape curve. The weight fraction of

Table 2. Quantitative X-ray diffraction results for the A1 specimens

Annealing time (min)	1275°C	1300°C	1325°C	1350°C
18	0	0	0	0
30	0	0	0	0
60	0	0	0	6.65
120	0	0	2.37	7.41
180	0	3.04	6.06	12.76
240	1.65	4.69	9.88	18.49
300	2.80	6.18	13.98	30.55
360	5.48	8.31	17.05	46.98
420	5.82	9.74	19.30	55.38
480	9.91	12.84	21.63	68.18
600	13.83	34.61	40.46	81.42
720	15.77	48.41	66.41	91.96
840	16.27	61.47	78.30	95.78
960	17.90	64.67	80.45	100
1440	30.55	74.85	85.04	100
1920	63.86	80.50	85.99	100

Table 3. Quantitative X-ray diffraction results for the C1 specimens

Annealing time (min)	1275°C	1300°C	1325°C	1350°C
18	0	0	0	3.15
30	0	0	0	3.44
60	0	0	0	11.08
120	6.52	7.89	8.69	28.86
180	7.22	12.38	22.83	52.04
240	7.94	16.80	43.16	73.71
300	18.29	26.71	53.15	73.86
360	19.73	27.57	53.95	75.05
420	20.73	38.26	55.06	78.68
480	43.83	51.24	58.52	79.10
600	47.76	54.80	60.79	84.02
720	49.27	58.20	76.31	85.65
840	57.64	59.33	82.33	86.79
960	61.60	63.00	87.02	88.85
1440	62.63	64.99	88.20	88.97
1920	65.12	74.00	88.50	89.85

cristobalite was plotted against the time, t , as shown in Fig. 3. At 1275°C, a lower reaction temperature, A1 specimens are in a fast transformation rate stage, whereas for specimens C1, a

typical S-curve is formed showing that the cristobalite addition in fused silica has a significant influence on the phase transformation of cristobalite. If the reaction temperature is above 1275°C, sam-

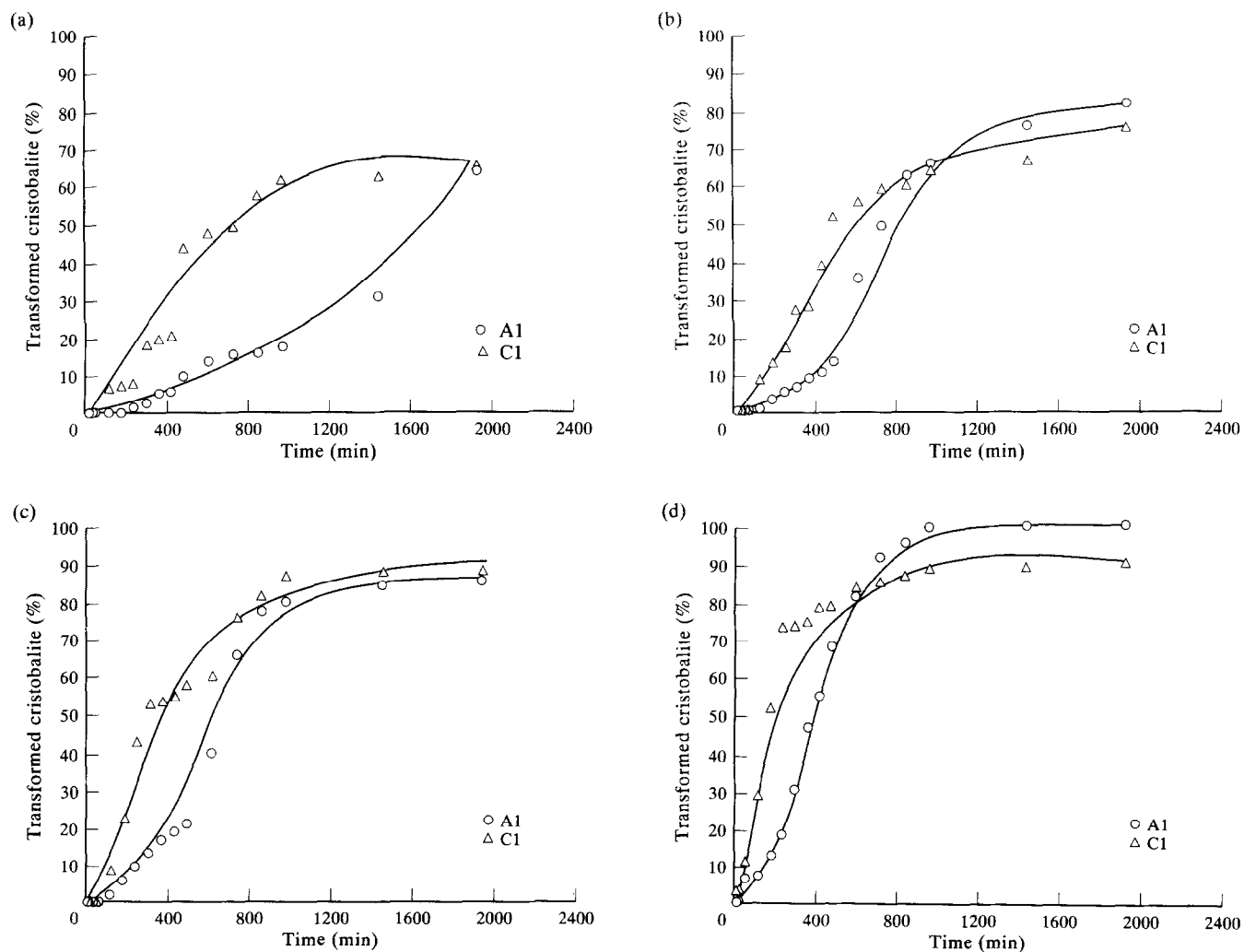


Fig. 3. The amount of transformed cristobalite as a function of time and composition at (a) 1275°C, (b) 1300°C, (c) 1325°C and (d) 1350°C.

ples with various compositions mostly display an S-curve. Therefore, the sigmoidal increase of weight percent of cristobalite with annealing time, t , can be fitted to a nucleation and growth kinetic model.⁷

3.1 Effect of composition on the reaction kinetics

The transformation rate of cristobalite from fused silica is shown in Fig. 3. The results indicate that the transformation rate is independent of composition at low temperature. However, the transformation of cristobalite is associated with the addition of cristobalite seeds at temperatures about 1325°C.

As can be seen, the dependence of crystallization of fused silica on composition is divided into two regions and related to soaking time at 1350°C. At the initial stage, namely shorter soaking time, the presence of cristobalite in the system assists the crystallization of fused silica as expected. Because the addition of cristobalite in fused silica acts as a seed for increasing the effective free surface and nucleation site, it would enhance the crystallization of fused silica. However, it significantly retards the crystallization as soaking time increases. It seems that cristobalite seed plays an important role in the crystallization of fused silica, which strongly depends on soaking time. A previous study,⁶ an investigation of the effect of zircon addition to fused silica, indicated that a compressive stress due to lattice distortion was induced on the surface region of fused silica particles, retarding the further crystallization of cristobalite. However, the X-ray slow rate scanning (0.03°/min) from 18° to 24° of 2θ , indicates that the interplanar spacing of the (101) plane of cristobalite does not change for specimens C1 by introducing cristobalite, as shown in Table 4. It seems that cristobalite seeds do not act in the same way as zirconium in silica.

The fused silica particle shaded area in Fig. 4 between two cristobalite particles is subject to compressive stress due to abrupt volume expansion during the cristobalite transformation from α phase to β phase at elevated temperature. A supplementary experiment was designed to simulate the mechanism and demonstrated the effect of stress on the inhibition of transformation from fused silica to cristobalite. The specimens shown

Table 4. The XRD results for specimens with various compositions reacted at 1350°C for 24 h

Composition	2θ (°)	$d_{(101)}$
Al	21.949	4.046
Cl	21.943	4.047

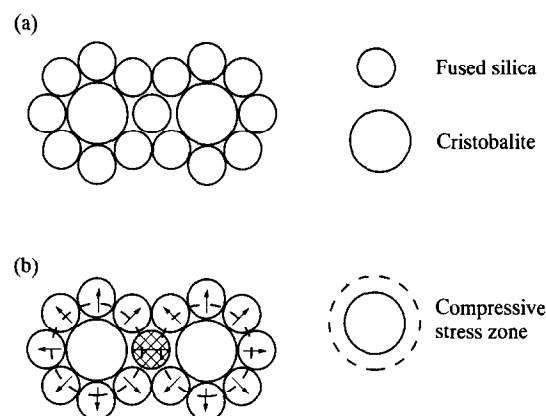


Fig. 4. Schematic diagrams showing the effect of cristobalite seeds on fused silica based materials: (a) initial state of raw materials; (b) reaction state of products.

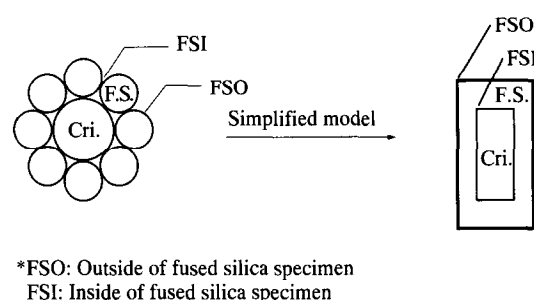


Fig. 5. Schematic diagram for simplified model with slip-casting experiment.

Table 5. XRD data of supplementary experimented specimens heated at 1350°C for 24 h

No.	2θ (°)	$d_{(101)}$	Integrated intensity (Counts)	Transformed rate (%)
FSO ^a	21.830	4.068	1186788	64.96
FSI ^b	21.749	4.083	917558	50.22
Cristobalite	21.946	4.047	1827071	100

^aFSO: Outside of fused silica specimens.

^bFSI: Inside of fused silica specimens.

schematically in Fig. 5 were formed by slip casting to conform free stacking of particles and sintered at 1350°C for 24 h. An X-ray diffractometer was used to determine the amount of transformation for fused silica outside surface layer (FSO) and interface layer (FSI) of particles. The results are listed in Table 5. The transformation rate of cristobalite in the interface layer is 15% lower than in the outside layer without contact with cristobalite, which demonstrates the inhibition effect of stress on transformation from α phase to β phase of cristobalite as predicted.

3.2 Cristobalite formation kinetics

At all temperatures the transformation is preceded by an incubation period. The incubation

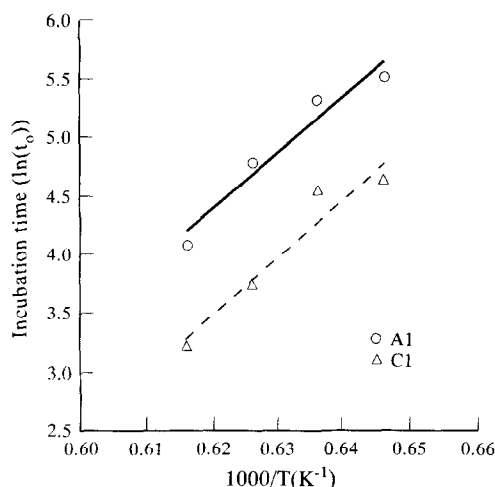


Fig. 6. Arrhenius plot of incubation time vs the annealing temperature gives the incubation energy Q : (a) 400 ± 10 kJ/mol for Al; (b) 414 ± 15 kJ/mol for Cl.

time, t_0 , was obtained by extrapolating the curve of the experimental results to a 2 wt% transformation level.⁹ The values of t_0 , plotted against transformation temperature in Fig. 6, suggest that the cristobalite incubation involves an activated process with an apparent activation energy, determining the temperature dependence of the diffusion and reaction processes which form cristobalite nuclei.

The results show that the incubation time decreases with the increase of reaction temperature only. The apparent activation energy Q with the values of 400 ± 10 kJ/mol and 414 ± 15 kJ/mol for specimen Al and Cl, respectively, is the same level for the activation process with and without the cristobalite additions. On the other hand, in Fig. 6, the Cl sample has a shorter incubation period than Al at all reaction temperatures. It seems that the cristobalite seed addition promotes the nuclei formation.

The nucleation and growth processes are expected to occur after the incubation stage, and can be described by a quantitative Avrami kinetic equation⁸⁻¹⁰

$$F(t) = 1 - \exp[-K(\dot{D})f(\dot{N}, \dot{G})t_m^n] \quad (1)$$

where $F(t)$ is the fraction of transformed cristobalite, $t_m = t - t_0$, where t_0 is the temperature-dependent incubation time. The term $K(\dot{D})$ is a constant that correlates the volume fraction to weight fraction. If the density of the parent phase is equal to the product phase, then $K(\dot{D}) = 1$.¹¹ The function $f(\dot{N}, \dot{G})$ depends upon the nucleation rate and the growth rate of the product, and n is the time exponent⁸ which is between 1 and 4, depending on the nucleation and growth mechanism and the crystal geometry.¹² A variety of similar equations can be described as follows

$$F(t) = 1 - \exp(-k_a t_m^n) \quad (2)$$

where $k_a = K(\dot{D})f(\dot{N}, \dot{G})$. The kinetic data in Fig. 3 can be fitted to eqn (2) in a linear form:

$$\ln(-\ln(1-F(t))) = \ln(k_a) + n \ln(t_m) \quad (3)$$

The values of n and k_a can be obtained from eqn (3) by plotting $\ln(-\ln(1-F(t)))$ vs $\ln(t_m)$ (Fig. 7). The values of n and k_a are obtained by measuring the slope and the intercept (by regression method), respectively. The values of the time exponents are between 1.63 and 0.74 as calculated. However, the transformation kinetics can be represented by a single line by subtracting out the incubation time, as shown in Fig. 7. The average time exponents, varying with composition, decrease with increasing cristobalite seed (e.g. additions of Al (1.446 ± 0.37); and Cl (0.951 ± 0.029)). The values of time exponents suggest that the transformation of pure fused silica is controlled by a long-range diffusion mechanism with two-dimensional plate-like growth. The cristobalite introduced may decrease

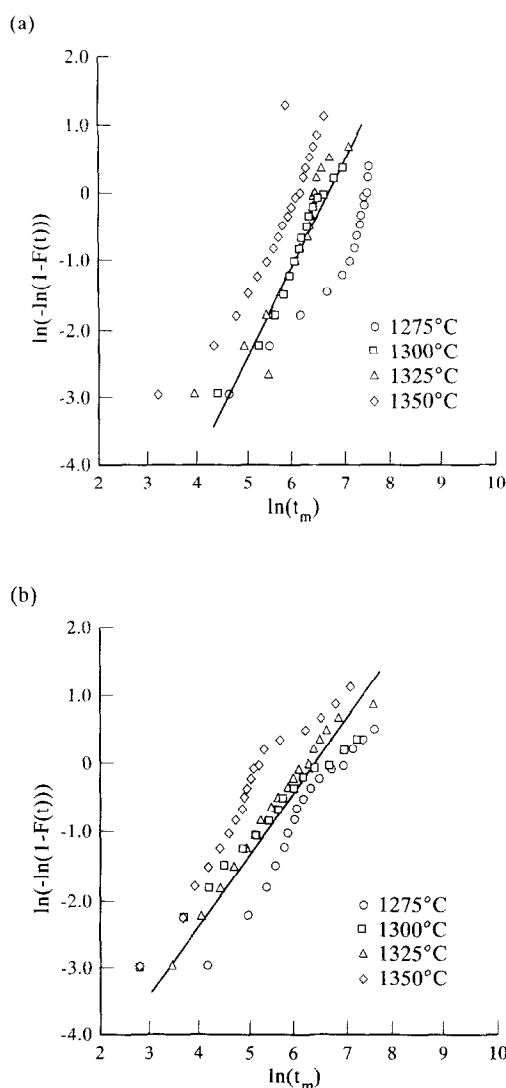


Fig. 7. Time exponent (n) of the cristobalite transformation plotted under normalized time and transformation weight scale. The average slopes, n , are: (a) 1.446 ± 0.37 for Al; (b) 0.951 ± 0.029 for Cl.

Table 6. Time exponent (n), k_a and $\log dF(t)/dt_{0.5}$ of cristobalite transformation of specimens AI and CI

Composition	Temperature (°C)	n	k_a	$\log (dF(t)/dt)_{0.5}$
AI	1275	1.052±0.058	2.084E-5	-3.319
	1300	1.634±0.025	3.053E-5	-3.193
	1325	1.588±0.048	3.230E-5	-3.000
	1350	1.510±0.015	1.151E-4	-2.876
CI	1275	1.076±0.043	6.067E-4	-3.651
	1300	0.740±0.007	1.978E-3	-3.280
	1325	0.997±0.020	3.857E-3	-2.954
	1350	0.991±0.059	7.620E-3	-2.786

the time exponent gradually with nearly one-dimensional needle-like growth.¹² However, the data shown in Fig. 7 are not a straight line, but rather a curve. The change in slope is attributed to the exhaustion of nucleation sites.¹¹ From Table 6, it also shows that the parameter k_a increases with increasing temperature as expected.

If eqn (2) is differentiated with respect to time, the rate of cristobalite transformation can be expressed as follows:

$$dF(t)/dt = k_a n t_m^{n-1} \exp(-k_a t_m^n) \quad (4)$$

The rate of transformation, $dF(t)/dt$, at different temperatures can be calculated by substituting into eqn (4) the known values n , k_a and t_m , which can be found from Table 6 and Fig. 3. On the other hand, the rate of transformation can also be expressed in Arrhenius form:¹²

$$dF(t)/dt = C \exp(-Q/RT) \quad (5)$$

where C is a constant depending on k_a , n and t_m^{n-1} , and Q is an apparent activation energy. Taking natural log on both sides of eqn (5).

$$\ln(dF(t)/dt) = -Q/RT + \ln C \quad (6)$$

By plotting $\log dF(t)/dt$ vs $1/T$, a straight line should be found. The slope of the line is given by $-Q/R$. Therefore, Q can be obtained by measuring the slope and multiplying by R . Figure 8 shows the result of plotting $\log (dF(t)/dt)$ vs $1000/T$ at 50% of transformed cristobalite. The activation energies for AI and CI were calculated as 126 ± 2 kJ/mol and 242 ± 7 kJ/mol, respectively. These values differ greatly from those obtained by calculating the incubation time. These results imply that the nucleation and growth process of cristobalite crystals is not similar to the incubation process of cristobalite nucleation in the solid-state reaction of the cristobalite-fused silica system. The activation energy of specimen CI is larger than that of AI series as predicted from Fig. 3. It is indicated that cristobalite seed addition results in a higher energy barrier for cristobalite transformation and that is the reason for the observed decreased transformation rate.

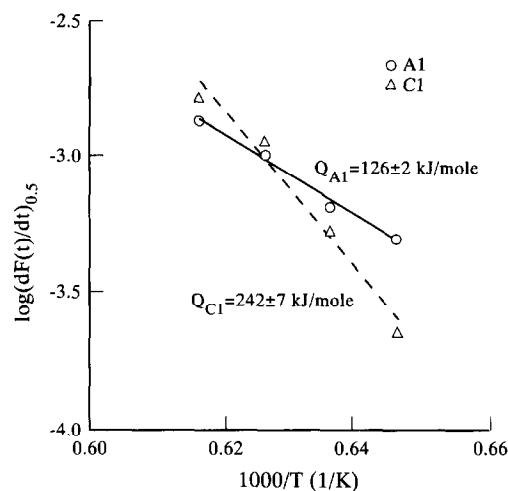


Fig. 8. $\log dF(t)/dt_{0.5}$ plotted against $1/T$ obtained by quantitative XRD for specimens AI and CI.

4 CONCLUSIONS

The transformation kinetics of fused silica based ceramic core with and without cristobalite seed addition for single-crystal casting application is determined by a quantitative X-ray diffraction analysis. The results can be summarized as follows:

- (1) A typical S-shaped curve can be fitted into a nucleation and growth kinetic model for fused silica-cristobalite transformation.
- (2) Cristobalite seed could affect the rate of transformation, which can be divided into two regions. At the initial stages, the presence of cristobalite seed assists the crystallization of fused silica because the cristobalite seed acts increasing the effective free surface and nucleation sites. However, it retards the crystallization as soaking time increases. The evidence shows that the cristobalite seed could induce the compressive stress from the abrupt volume expansion of cristobalite transformation from α phase to β phase at elevated temperature.
- (3) There is an incubation time before the transformation starts. The incubation is

an activated process with an apparent activation energy of 400 ± 10 kJ/mol and 414 ± 15 kJ/mol for specimens Al and Cl, respectively.

- (4) The transformation kinetics measured by quantitative X-ray diffraction can be fitted to an Avrami equation with a time exponent between 1.45 and 0.95 for specimens with different compositions. It is observed that the time exponent, n , decreases with increasing cristobalite seed addition. The results of time exponents suggest that the transformation kinetics is controlled by a long-range diffusion mechanism changing the two-dimension plate-like growth to one-dimensional needle-like growth.

REFERENCES

1. WANG, L.-Y. & HON, M.-H., The role of vinyl tris(2-methoxyethoxy)silane in the suspensions of fused silica-polypropylene-wax for ceramic injection molding. (To be published.)
2. HUSEBY, I. C., BOROM, M. P. & GRESJKOVID, C. D., High temperature characterization of silica-base core for superalloys. *Am. Ceram. Bull.*, **58** (1979) 448-52.
3. KATO, K. & NOZAKI, Y., Ceramic core for precision castings manufactured by injection molding. *Imono*, **63** (1991) 155-60.
4. KATO, K. & NOZAKI, Y., Ceramic core for solidification controlled casting. *Imono*, **62** (1990) 726-31.
5. TAKAYANAGI, T. & KATASHIMA, S., Crystallization of the fused silica flour used to make ceramic core at elevated temperatures. *Imono*, **60** (1988) 401-6.
6. MILL, D. & CHEM, C., Properties of ceramic core. *The British Investment Casters' Technical Association 15th Annual Conf.*, Torquay, 29 April-1 May (1979) Paper 7: 1-7: 14.
7. WANG, L.-Y. & HON, M.-H., The effect of zircon addition on the crystallization of fused silica — a kinetic study. *J. Ceram. Soc. Jpn.*, (submitted).
8. AVRAMI, M., Kinetics of phase change. I. General theory. *J. Chem. Phys.*, **7** (1939) 1103-12.
9. AVRAMI, M., Kinetics of phase change. II. Transformation-time relations for random distribution of nuclei. *ibid.*, **8** (1940) 212-24.
10. AVRAMI, M., Kinetics of phase change. III. Granulation, phase change, and microstructure. *ibid.*, **9** (1941) 177-84.
11. WEI, W. C. & HALLORAN, J. W., Transformation kinetics of diphasic aluminosilicate gels. *J. Am. Ceram. Soc.*, **71** (1988) 581-7.
12. RAO, C. R. N. & RAO, K. J., *Phase Transformation in Solid*. McGraw-Hill, USA, 1978, p. 93.